

Evaluating sealability of blended smart polymer and fiber additive for geothermal drilling with the effect of fracture opening size

Musaab Magzoub^a, Tobenna Anyaezu^a, Saeed Salehi^{a,*}, Guoqiang Li^b, Jizhou Fan^b, Catalin Teodoriu^a, Fatemeh K. Saleh^a, Arash Dahi Taleghani^c

^a University of Oklahoma, USA

^b Louisiana State University, USA

^c Penn State University, USA

ARTICLE INFO

Keywords:

Shape memory polymer (SMP)
Sealability
Lost circulation
Geothermal drilling

ABSTRACT

Geothermal formations often contain extensive fracture networks. These fracture networks contribute to the significant loss of drilling fluids during geothermal drilling. Multiple loss circulation materials (LCM) such as fiber, granules, and pills have been proposed to tackle this problem but with only limited success. Recent advances in materials science have led to the development of thermoset shape memory polymers (SMP) to address the lost circulation problem. In this paper, we evaluate a thermoset SMP performance in sealing near wellbore fractures of different sizes in geothermal wells. The SMP performance was assessed using granite disks and cylindrical granite cores having fracture sizes of 1000 μm and 3000 μm . A static filtration test was performed using cedar fiber, CaCO_3 , and SMP. Results showed cedar fiber performed better than the CaCO_3 , reducing fluid loss by 89% and improving sealing pressure by 200 psi. A novel dynamic testing unit that allows for high-temperature testing under flowing conditions was used in this study. The analysis showed that 3% by weight SMP and fiber blends could bridge and plug the 1000 μm fracture. For a larger fracture of 3000 μm width, there was a need to increase the weight concentration of the SMP to 6% to plug the fracture opening effectively. We showed the influence of key parameters such as the type of LCM, concentration, and particle size distribution in optimizing the performance of drilling fluid loss treatment.

1. Introduction

Lost circulation continues to be a significant problem during geothermal drilling. From an economic perspective, the loss of drilling fluids to the formation and the non-productive time (NPT) spent trying to solve these problems is one of the most costly and undesired encounters in the petroleum industry. Besides, the technical and operational challenges faced in solving lost circulation in geothermal wells pose more economic concerns. Drilling a geothermal well typically costs between 30 and 50% of hydrothermal/geothermal projects and more than half of the cost of Enhanced Geothermal Systems (EGS) (Dumas et al., 2013). In general, lost circulation account for 10–20% of the cost of the geothermal wells, roughly 3.5–10% of the capital of a geothermal project (Finger and Blankenship, 2010). In a recent study, it was estimated that lost circulation accounted for US\$2–\$4 billion annual costs due to NPT. Moreover, the uncontrolled loss of fluid can damage the

reservoir's formation and have an adverse effect on its production potential (Cook et al., 2012). If this problem continues, losses will lead to other drilling problems such as differential sticking, well control problems, and poor hole cleaning.

In the Gulf of Mexico, lost circulation, stuck pipe, and wellbore collapse, which are common problems associated with lost circulation, account for 44% of the total NPT. Also, losing a large amount of the synthetic-base muds usually used in these operations can be costly. The cost of synthetic-base muds ranges from \$100 to \$200 per barrel in addition to the cost of lost circulation materials (LCM). Innovative solutions and engineered LCM such as the shape memory polymers (SMP) that are proposed in this study can significantly reduce lost circulation problems and overcome many of the operational limitations in high-temperature conditions or deep wells, usually faced in geothermal drilling. Even though the cost of SMP are slightly higher than commercial LCM types, they could be more effective in low concentration compared to the conventional LCM. These SMPs can efficiently bridge

* Corresponding author.

E-mail addresses: magzoub@ou.edu (M. Magzoub), tobennaanyaezu@ou.edu (T. Anyaezu), salehi@ou.edu (S. Salehi), guoqi1@lsu.edu (G. Li), jfan6@lsu.edu (J. Fan), cteodoriu@ou.edu (C. Teodoriu), Fatemeh.Karbalaei.Saleh-1@ou.edu (F.K. Saleh), aud440@psu.edu (A.D. Taleghani).

<https://doi.org/10.1016/j.petrol.2021.108998>

Received 24 January 2021; Received in revised form 6 May 2021; Accepted 23 May 2021

Available online 30 May 2021

0920-4105/© 2021 Published by Elsevier B.V.

Acronyms

CF	cedar fiber
EGS	enhanced geothermal systems
LCM	lost circulation material
SMP	shape memory polymers
PPA	permeability plugging apparatus

and seal the fractures, preventing mud loss and excessive costs. Moreover, recent studies showed that the synthesis of SMP from novel polymeric materials with thermally induced shape memory properties could be a potential candidate with high shape recovery, low cost, and easy manufacturing process (Lendlein and Kelch, 2002; Liu et al., 2014; Mudgal and Ghorai, 2015).

On the other hand, appropriate well planning, understanding the root cause of the losses, and identifying the location where the loss occurs are important in curing the loss. A comprehensive understanding of lost circulation requires knowledge of the formation's mechanical properties such as near-wellbore stresses, pore pressure, Poisson's ratio, and the physical and chemical properties of drilling fluids and their interactions (Feng and Gray, 2018).

Most lost circulation incidents are caused by open fractures extending far deep into the formation as well as reopening of existing and natural fractures by high bottomhole pressure. One of the problematic situations of lost circulation in geothermal wells is the cross-flow between permeable zones with different pressures. An example of this situation is alluvial deposits that are separated by an impermeable layer from underlying volcanics. Significant loss occurs when the drilling penetrates the volcanics (Bauer et al., 2005). One of the effective treating or preventing methods is wellbore strengthening. Wellbore strengthening can be defined as techniques used to increase the pressure that a wellbore can withstand before fracturing and eventually causes fluid loss into the formation. Wellbore strengthening aims to artificially improve the breakdown pressure and expand the drilling mud window. Salehi and Nygaard (2011) reviewed existing wellbore strengthening models and found that the formation fracture gradient can increase considerably by enhancing fracture propagation pressure. Wellbore strengthening involves sealing or plugging wellbore fractures with lost circulation materials (LCMs) to stop drilling fluids' continuous loss. The best method employed in dealing with lost circulation is to prevent it from happening with appropriate well planning.

Conventional LCMs were initially categorized based on their appearance as flaky, fibrous, granular, and a mix of two or all three. Alsaba et al. (2014) proposed an updated LCM classification based on their physical properties, chemical properties, and applications. The physical properties included the appearance and particle size, while the

chemical properties included acid solubility, swellability, and reactivity with other chemicals or activation. LCMs are reclassified as flaky, granular, acid-soluble, fibrous, LCMs mixture, high fluid loss squeeze (HFLS), nanoparticles, and swellable/hydratable LCMs. Table 1 lists examples of LCMs that can be used for lost circulation treatment.

Loss circulation treatments can be either preventive or remedial. Preventive lost circulation treatment involves anticipating mud loss and treating the drilling fluid with lost circulation pills. Remedial lost circulation consists of treating the drilling fluid only after a loss has occurred. LCMs can be added to the drilling mud continuously or intermittently as a spotted pill. More importantly, experimental testing of LCMs is essential before being deployed for field usage. Testing LCM in controlled laboratory conditions allows companies to fully understand how the materials will function in the operating conditions. Several researchers have recommended and examined different types of materials, including cellulosic fibers (Fridheim et al., 2012), particulate matter and granules (Ekeoma et al., 2019), nanoparticles (Contreras et al., 2014), and crosslinked polymers (Magzoub et al., 2020). However, selecting proper LCM for geothermal application is limited by the temperature constraints, in addition to the large fractures that usually exist in geothermal reservoirs (Lee and Taleghani, 2020). The challenges in addressing the lost circulation in geothermal drilling lie in the temperature effect on the properties of the drilling fluid and LCM. Most conventional materials degrade under high temperature in addition to the mud flocculation effects that affect the ability of mud to hold large size particles required to seal large fractures (Mietta et al., 2009). One of the available options for high-temperature drilling is to use materials such as thermoset rubbers, ground coal, mineral fibers, and modified polymers (Brandl et al., 2011; Loeppke, 1986). Some studies revealed that the performance of drilling fluid could be enhanced by adding high-temperature-resistant materials such as strata-wool and mineral fibers (Loeppke, 1986; Salih and Bilgesu, 2017). Recent studies suggested using silicon nanoparticles that have high thermal stability up to 2500 °F (1370 °C) (Javeri et al., 2011). Bauer et al. (2004) investigated the potential utilization of plugging materials comprised of polymers and silicates that can be integrated into high-temperature grout systems. The authors studied the system's stability and demonstrated that it is hydrolysis resistant for at least 8 weeks at 350 °F. The system can be a good candidate for treating lost circulation in geothermal drilling.

Despite the variety of materials suggested for lost circulation treatment in geothermal drilling, there are still some operational limitations in deep wells due to the pumping difficulties and size of bit nozzles (Magzoub et al., 2021a, b). Ezeakacha and Salehi (2019) conducted an experimental study to evaluate the effect of particle size and operational parameters in the dynamic filtration under a temperature range from 120 to 240 °F (50–115 °C). The results demonstrated that LCM concentration and temperature greatly influence filtration, which may pose some limitations in deep drilling. Moreover, the study also revealed that increasing the temperature from 120 °F (50 °C) to only 220 °F (105 °C)

Table 1
Examples of different types of lost circulation materials.

Classification	LCM Examples	Temperature range	Reference(s)
Low temperature	Calcium carbonate, walnut, and nutshell.	Mostly works at low temperature, less than 120 °F (50 °C)	Alsaba et al. (2014)
	Cellophane, cottonseed hulls, and mica.	Low to elevated temperatures, less than 300 °F (150 °C)	Alsaba et al. (2014)
	Cedar fiber, mineral fibers, sawdust, shredded paper, and natural cellulose fiber.	Low to elevated temperatures, less than 300 °F (150 °C)	Alsaba et al. (2014)
High temperature	Nanoparticles of silicon, iron hydroxide, or copper oxide.	Wide temperature range. More than 300 °F (150 °C)	Contreras et al. (2014)
	Hydrophobically modified polysaccharide	400 °F (205 °C)	Brandl et al. (2011)
	Strata-wool and mineral fibers	480 to 1040 °F to (250–560 °C)	Salih and Bilgesu (2017)
	Thermoset polymers, swellable clays, and encapsulated cross-linkable polymers.	Wide temperature range. More than 300 °F (150 °C)	Mansour et al. (2019) Zhong et al., 2019)
	Thermoset Rubber	Up to 200 °F (95 °C)	Hamza et al. (2019)
Coal	250 to 330 °F (121–165 °C)	Loeppke et al. (1990)	
Polyacrylamide crosslinked with polyethyleneimine, chromium acetate, or chitosan.	High thermal stability. Works at low and high temperature, more than 300 °F (150 °C)	Loeppke et al. (1990)	
			Hamza et al. (2019)

significantly impacted the dynamic mud filtration. It masked the positive effect of increasing LCM concentration from 30 lb/bbl to 80 lb/bbl (Ezeakacha and Salehi, 2019). These challenges in selecting the proper size, type, and concentration of LCM for geothermal drilling urged the need for innovative materials such as shape memory polymers. (Ezeakacha and Salehi, 2019).

Recently, Mansour et al. (2019) suggested using expandable shape memory polymers (SMP) in curing lost circulation problems and strengthening the wellbore. The SMP is a smart polymer that is thermally activated and functions as an LCM when added to drilling mud to plug lost circulation zones. The SMP can be activated at certain temperatures and programmed to take different shapes based on the fracture size to be plugged (Mansour and Taleghani, 2018). In a similar application, Dahi Taleghani et al. (2017) presented the potential application of SMP as an effective expansive cement additive. They applied SMP in a controlled expansion of the cement slurry in preventing cementing channeling, debonding, and fluid migration (Mansour et al., 2019). Experiments are usually conducted with a permeability plugging apparatus (PPA). The performance of LCM is evaluated based on the fluid loss through the fractures, time required for a seal to build across the fracture, and maximum sealing pressure across the fracture face.

1.1. Geothermal reservoirs fracture characterization

Geothermal formations vary from one location to another and may contain granite, granodiorite, quartzite, greywacke, basalt, and volcanic tuff. Of all these lithologies, granite is the most frequently occurring rock type (Gianelli et al., 1997; Schild et al., 1998; Villa et al., 2006). The complexity of geothermal lithologies is the primary contributor to mud loss events while drilling. Geothermal wells contain natural fractures and cavernous rocks with vuggy pores. While these fractures contribute to lost circulation, they also enable the production of geothermal fluids.

Characterization of fractures is important, especially in fractured reservoirs, as seen in geothermal wells. According to Seifollahi et al. (2014), fracture geometries and the number of fractures are two critical parameters used in characterizing fracture networks. Topological and metric properties are two divisions of fracture geometry as a parameter. The measured properties include but are not limited to fracture length, aperture, spacing, and orientation (Singhal and Gupta, 2010). The topological properties include the fractures' connectivity (Jing and Stephansson, 1997). Hanano (2000) characterized fracture sizes and permeabilities in geothermal wells and highlighted two different roles of fractures in geothermal wells; one is the contribution to the convection in geothermal systems, and the other is connecting the well to the reservoir to increase the production. In geothermal systems such as the EGS, the feasibility of the energy project and efficiency of heat extraction depends on the ability to create and maintain open fracture networks (Dobson et al., 2021).

In a different study by Vidal et al. (2017), the authors highlighted the importance of fracture sizes (shape, aperture, width, height, and length) and fracture properties (thickness, offset, horizontal trace, density, and permeability). The authors correlated fracture length to the severity of mud loss in their modeling study. Therefore, for lost circulation rates greater than or equal to $10 \text{ m}^3/\text{h}$ ($353 \text{ ft}^3/\text{h}$), the permeable fractures are developed with a 100 m (328 ft) diameter. If the loss rate is less than $10 \text{ m}^3/\text{h}$ ($353 \text{ ft}^3/\text{h}$), the permeable fractures are modeled with a 69.8 m (229 ft) diameter. Permeable zones without drilling fluid losses but correlated temperature anomalies are modeled with a fracture of 50 m (164 ft) diameter. The three classes/sizes of fractures were used as geometric constraints for the connections not directly observed between fracture zones and the well.

2. Materials and experimental methodology

2.1. Materials

The SMP utilized in this study is a temperature-activated polymer. The SMP was synthesized out of a readily available commercial epoxy resin (EPON 826, a bisphenol A based resin) cured by an isophorone diamine (IPD) crosslinker. Each 100 g EPON 826 was bonded with 23.2 g IPD to balance out the stoichiometry. The reagents were blended by a mechanical mixer for 2 min at ambient temperature and then placed inside a cylindrical silicone mold with a diameter of 1 inch and a height of 0.5 inches. The air bubbles were separated by vacuum at room temperature. After 1 h of curing at a temperature of 300°F (150°C), a thermoset network was achieved. Each cylindrical sample was uniaxially compressed at 320°F (160°C) until some crack appeared (around 45% of compressive strain), and the strain was held constant while cooling down to room temperature, followed by removal of the compressive load. This completed hot programming of the SMP. After that, the SMP was shattered into pieces and crushed again by a press into smaller-sized grains. These crushed grains were milled by the PQ-N2 planetary ball mill machine (Across international). For every half hour, the ball milling machine was halted and sieved into obtaining different-sized particles, ranging from a few millimeters to fine powders. The particle sizes were 0.6 mm–2.14 mm. The thermo-mechanical properties of the high enthalpy storage thermoset SMP include high compressive strength of 320 MPa and high stiffness of 1.05 GPa at 70°F (21°C), a glass transition temperature of 300°F (150°C) and rendering high recovery stress of 17 MPa, and energy output of $2.12 \text{ MJ}/\text{m}^3$ in its rubbery state and bulk form (Fan and Li, 2018). Fan et al. (2020) also used the same SMP as an additive compound to cement paste at a ratio of 1, 2, 4, and 6% by weight of cement. They found that the circumferential expansion ratio of the cement G composite can get to 1.4% by adding 6% by weight of EPON-IPD particles. As shown in Fig. 1, A and A' are the digital photo and scanning electron microscopy images of the power additive, and B and B' are the digital photo and optical microscopy images of the particle additive. The granular SMP was chosen in this study because the sealing of the fracture requires larger particles to form the plug, while fine particles are limited to controlling the filtration at the pore scale.

In this study, in addition to the SMP, two other commonly used LCMs were chosen to evaluate their sealing efficiency, calcium carbonate CaCO_3 and Cedar Fiber (CF). A water-based (WBM) mud was prepared with 20 lb/bbl bentonite as viscosity additive, 4 lb/bbl caustic soda for pH, and 4 lb/bbl lignite as a deflocculant for proper dispersions of solids in the mud. Four different formulations were used, includes the two selected conventional LCMs and SMP as follows: (1) 55 lb/bbl of CaCO_3 , (2) 5 lb/bbl of cedar Fiber, (3) 3% SMP, and (4) combination of 3% SMP and 5 lb/bbl of cedar fiber.

2.2. Experimental methodology

Sealing experiments were conducted in static and dynamic conditions. Table 2 shows a list of the conducted experiments and their testing conditions. The size of fractures was selected based on two bases, first to investigate the effect of fracture size on the performance of the SMP, second is to simulate the actual fractures that exist in geothermal drilling. According to Miranda et al. (2018), minor losses are caused by fractures having apertures less than $100 \mu\text{m}$, while severe loss is usually encountered in formations having fractures ranging from $100 \mu\text{m}$ to $10,000 \mu\text{m}$. The characterization study of fracture networks conducted by Miranda et al. (2018) on geothermal data also showed that the fracture lengths vary from 1.3 ft to 32 ft (0.4 m–10 m) (Miranda et al., 2018). In this study, various 13.5-inch-long fractures were prepared with a fracture aperture of $1000 \mu\text{m}$ and $3000 \mu\text{m}$.

For the static condition testing, a permeability plugging apparatus (PPA) was used. The PPA is equipped with a fractured carbonate disk

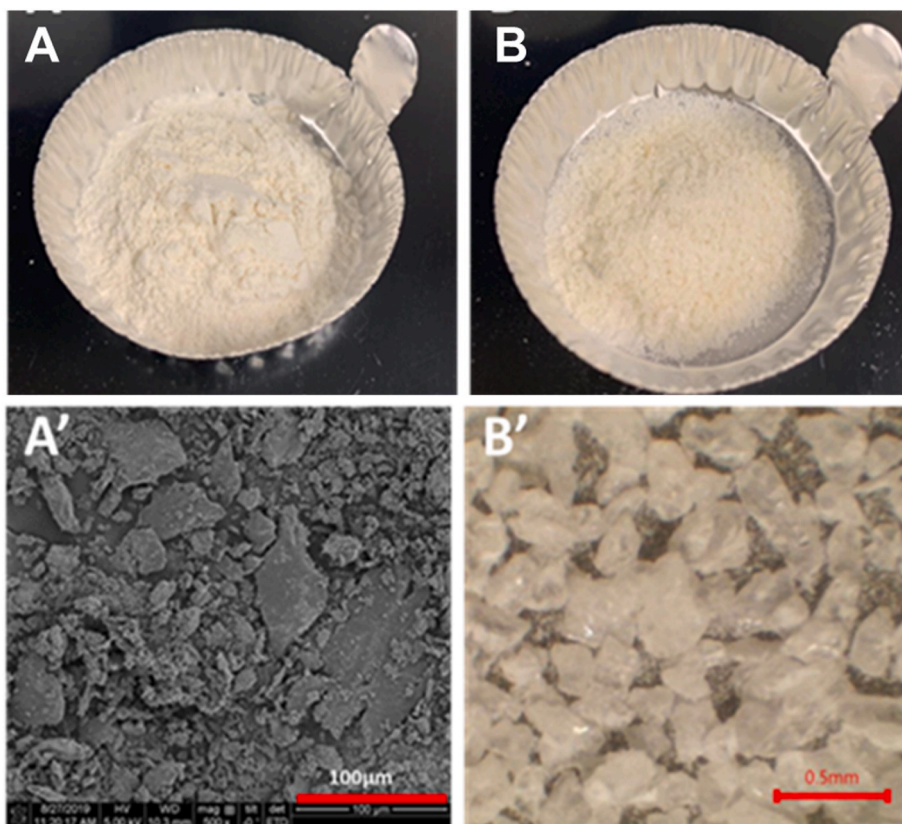


Fig. 1. The powder additive: A - digital photo and A' - scanning electron microscopy (SEM) images; and the particle additive: B - digital additive and B' - optical microscopy images.

Table 2

List of conducted experiments and their testing conditions.

Type of the filtration test	Fracture dimensions	LCM type and concentration	Temperature and pressure
Static	Width = 1000 µm height = 1 inches (25.4 mm) length = 0.25 inches (6.35 mm)	55 lb/bbl CaCO ₃	300 °F
		5 lb/bbl cedar fiber	500 psi differential pressure
		5 lb/bbl cedar fiber +3 wt% SMP (11 lb/bbl)	
Dynamic	Width = 1000 µm height = 1 inches (25.4 mm) length = 13.5 inches (34.3 cm)	55 lb/bbl CaCO ₃	300 °F
		5 lb/bbl cedar fiber	50 to 500 psi differential pressure
		3 wt% SMP (11 lb/bbl) 5 lb/bbl cedar fiber +3 wt% SMP (11 lb/bbl)	
	Width = 3000 m height = 1 inches (25.4 mm) length = 13.5 inches (34.3 cm)	5 lb/bbl cedar fiber	
		+3 wt% SMP (11 lb/bbl)	
		5 lb/bbl cedar fiber +6 wt% SMP (11 lb/bbl)	

having a fracture of 1000 µm opening is shown in Fig. 2. The granite disks were used instead of the conventional aluminum disk to represent actual downhole rocks where the thermal conductivity of the rock may affect the activation of the SMP. The test is conducted by applying a differential pressure of 500 psi at 300 °F (150 °C) for 30 min, and during that, the cumulative filtrates sealing pressure were recorded.



Fig. 2. Static filtration experimental setup, PPA with the fractured disk.

For the dynamic filtration, a newly designed high-temperature dynamic LCM testing apparatus was used to investigate the fracture sealing efficiency of all four LCMs blends. Magzoub et al. (2021a, b) showed that this innovative high-temperature dynamic fracture testing apparatus improves testing conditions compared to the conventional permeability plugging apparatus (PPA). The testing unit provides a method for large-scale dynamical testing of LCMs with circulating drilling fluid. Figs. 3 and 4 show a photo and sketch of the testing unit. The setup consists of three major systems: the circulation system, core system, and mud loss collection system. The circulation system is using a positive displacement pump with five speeds controller to gives a flow rate of

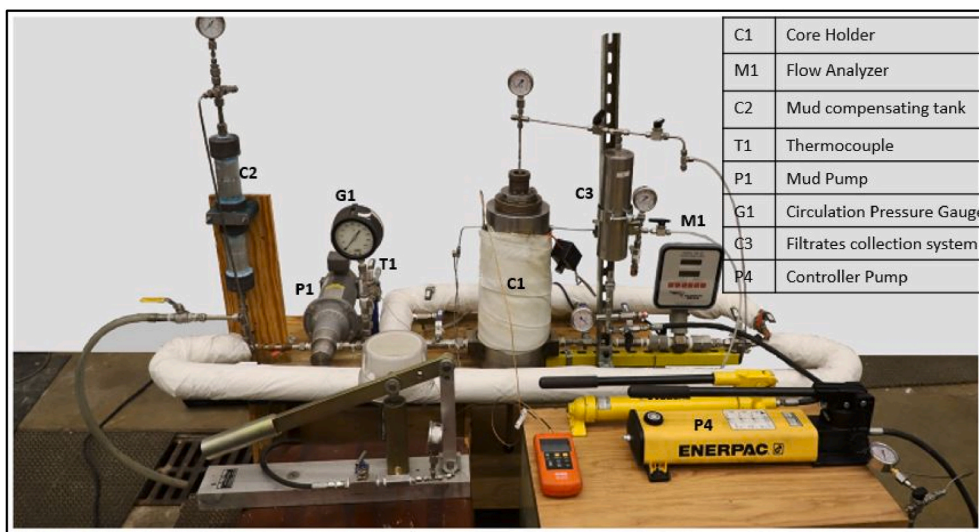


Fig. 3. High-temperature dynamic LCM testing Setup (Modified from Magzoub et al. (2021a, b)).

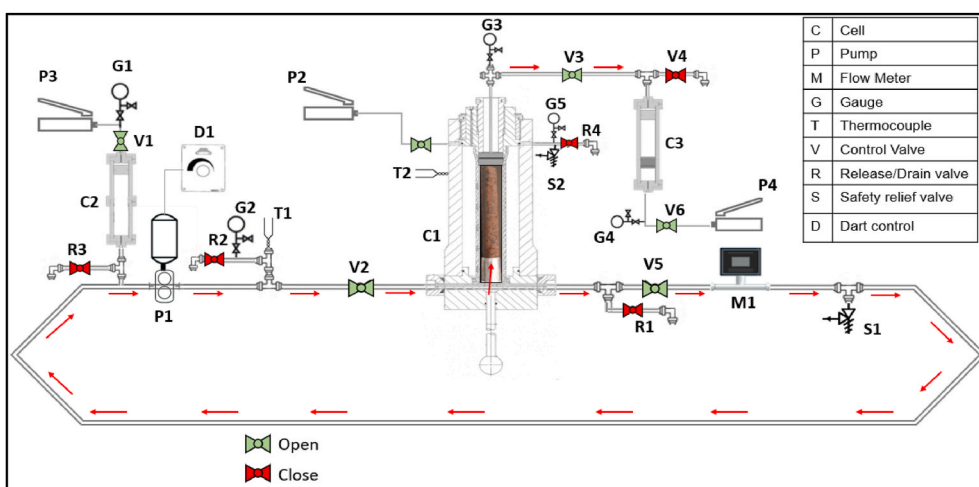


Fig. 4. Sketch of the high-temperature dynamic LCM testing unit with the core sample inserted in the cell. (Magzoub et al. (2021a, b)).

2–4.5 gpm (7.5–17 l/min). The total volume inside the loop is 1200 cm³. The main loop allows filtrates to pass through the fracture, while the bypass loop is used for conditioning the mud to the desired temperature before the test. The main circulation loop is 160 inches (406.4 cm) in length and having a diameter of about 0.5 inches (1.27 cm). The circulating system mainly consists of a mud compensating tank, mud pump, pressure gauges, flow analyzer, and thermocouples. The confining cell can accommodate a 2.5 × 14 inches core sample. The setup is equipped with a mud loss collection cell, a set of hydraulic pumps, heating belts, thermocouples, and gauges. This approach applies differential pressure through the core sample by circulating the drilling fluid comprising the shape memory polymers within the pressurized flow loop. The circulation rate is held steady as the temperature is gradually increased to 400 °F (205 °C), and pressure is increased stepwise from 100 to 500 psi. The experimental apparatus permits the collection of filtrates each minute while observing the sealing pressure.

The study’s objective is to assess the shape memory polymer’s sealing efficiency in plugging 1000 μm and 3000 μm fractures. The continuous fluid circulation through the flow loop simulates the drilling fluid circulation in a wellbore. An open fracture is identified by pressure communication before and after the core sample. The LCM in the flowing drilling mud will develop the bridge to seal the fracture opening.

During this process, any filtrate that evades the entire core length will be amassed inside the collection pressure vessel installed after the fracture. The differential pressure across the fracture opening will be deemed as the sealing pressure. Experiments with the dynamic high-temperature apparatus are challenging, costly, and time-consuming. Therefore, a test with water-based mud (WBM) was repeated for data reproducibility and error estimation. The measurement error on the aggregate filtrates and sealing pressure ranged between 5 and 10%, and sealing pressure averaged less than 5%.

2.3. Granite cores preparation

Granites are common geothermal reservoir rocks; the samples used in this study were obtained from the Oklahoma area. Two types were collected, the Georgia gray granite and the Oklahoma reddish granite, as shown in Figs. 5 and 6. For the static filtration, 0.25 × 2.5 inches granite disks were prepared, as shown in Fig. 5, while the dynamic filtration with the high-temperature dynamic setup required a core of 2.5 × 13.5 inches. Two different fracture widths were prepared with a width of 1000 μm and 3000 μm along the whole core length, as shown in Fig. 6. To prepare long-fracture cores, the cores were initially cut into two halves. Then an aluminum sheet was used as a spacer to model the



Fig. 5. (Right) Granite disk, 2.5" Di x 0.25" thickness, (Left) Same disk with a fracture of 1" length x 1000 μm width.



Fig. 6. A core with O.D. of 2.5 in and length of 13.5 in with longitudinal and cross-sectional views of the fracture with the width of 1000 μm.

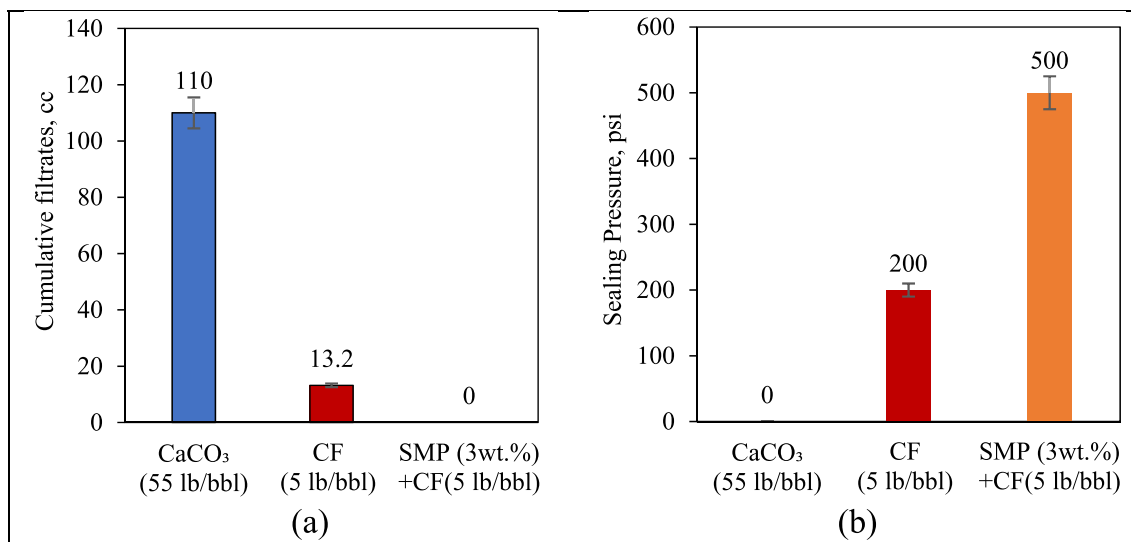


Fig. 7. Static filtration results showing (a) cumulative 30-mins filtrates and (b) sealing pressure. Tests conducted at 300 °F (150 °C) for CF and SMP + CF, and at 120 °F (50 °C) for CaCO₃.

fracture width presented before welding the two halves together with a high-pressure, high-temperature glue.

3. Results and discussion

3.1. Static filtration experiments

Static filtration provides a basic evaluation of the performance of LCM in fracture sealing under HPHT conditions. Many factors could affect the performance of LCM, such as types, concentration, and particle size. To quickly evaluate SMP's performance compared with the selected commonly used LCM, static filtration tests were conducted for different formulations of LCM in WBM. After conditioning the samples to the required pressure and temperature, upstream pressure and filtration volumes were documented.

The maximum stable pressures across the granite disk after the static filtration tests were considered to be the sealing pressure. Fig. 7a and b shows the results for the calcium carbonate cedar fiber and SMP + fiber blends tested at 300 °F (150 °C) and for the calcium carbonate tested at 120 °F. The calcium carbonate at elevated temperature attained no sealing pressure (0.0 psi) when tested with the 1000 μ m disk. Also, high cumulative filtration (110 cc) was observed. On the other hand, the sealing pressure for the plugs formed by the fiber was 200 psi, which reduced the filtration from 110 cc to 13.2 cc. Furthermore, introducing the SMP to the WBM with fiber greatly improved the loss control and stopped fluid loss with the maximum sealing equal to the maximum applied differential pressure (500 psi) during the PPA test.

3.2. Dynamic flow loop simulator

3.2.1. Sealing integrity in a 1000 μ m fracture

The dynamic fluid loss testing gives a more reliable assessment of the fracture sealing process. This section presents the results of the dynamic high-temperature fluid loss experiments using the 1000 μ m fracture created in the 2.5in \times 13.5in granite cores. The progress of mud loss with time for the four different LCM blends (CaCO₃, CF, SMP, and SMP + CF) is presented in Fig. 8. The tests started with 100 psi circulating pressure and increased stepwise every 5 min. The results show how mud loss depended on the type of LCM used. For instance, as soon as the circulating pressure increased to 100 psi, the drilling fluid containing

CaCO₃ exhibited a sudden and severe loss, which continued for 5 min accumulating about 65 cc mud loss.; this is equivalent to 3.6 vol% of the system's total mud. Conversely, cedar fiber (CF) showed excellent performance at a differential pressure less than 400 psi; the mud loss was not significant (less than 10 cc) until the circulation pressure of 400 psi is reached. Beyond this pressure, a progressive mud loss was observed, which took more than 10 min to reform the plug after losing a total of 150 cc, equivalent to 8.3% of the mud in the flow loop.

The mud loss profiles presented in Fig. 8 also demonstrate the superior performance of the mud containing 3 wt% of SMP. The SMP in this concentration succeeded in stopping the mud loss through the 1000 μ m fracture for the circulating pressure starts from 100 to 500 psi. However, the mud loss with the 3 wt% SMP started when a pressure of 200 psi was exceeded, but the loss rate (15 cc/min) was significantly less than the loss exhibited with the CaCO₃. The increase in loss with time was proportional to the circulation pressure. After about 10 min from the start of the loss, the SMP seemed to form an adequate plug on the fracture opening indicated by the stop of the loss, which peaked at 160 cc. The loss stopped due to the creation of the sealing by the activated particles of the SMP, which expanded when activation temperature, 300 °F (150 °C) was attained. Furthermore, testing with SMP + CF blend shows a significant reduction in mud loss by more than 95%. No loss was observed below 300 psi circulating pressure, and the loss peaked at 10 cc till the end of the experiment.

The loss rate directly depends on the sealing pressure provided by the plug. The loss rate will be lower if the plug is created faster, depending on the type of LCM used in the mud. Fig. 9 summarizes the recorded sealing pressure during the stepwise circulating pressure increasing. The four types of mud yield different sealing pressure depending on the mechanism of bridging with different LCM used. For instance, the mud containing CaCO₃, which produced high mud loss as demonstrated above in Fig. 8, also showed very low sealing pressure, less than 50 psi, at 300 °F (150 °C). This was verified during the test by increasing the circulating pressure while observing the pressure across the fracture, where the plug created by the CaCO₃ could not withstand more than 50 psi. As a result of this low sealing pressure, severe mud loss was continued until total loss occurred at a differential pressure of 300 psi. The sealing pressure results explain the total loss because the sealing integrity was not maintained. For the CF, the sealing pressure was maintained while the plug been intact until 300 psi circulating pressure

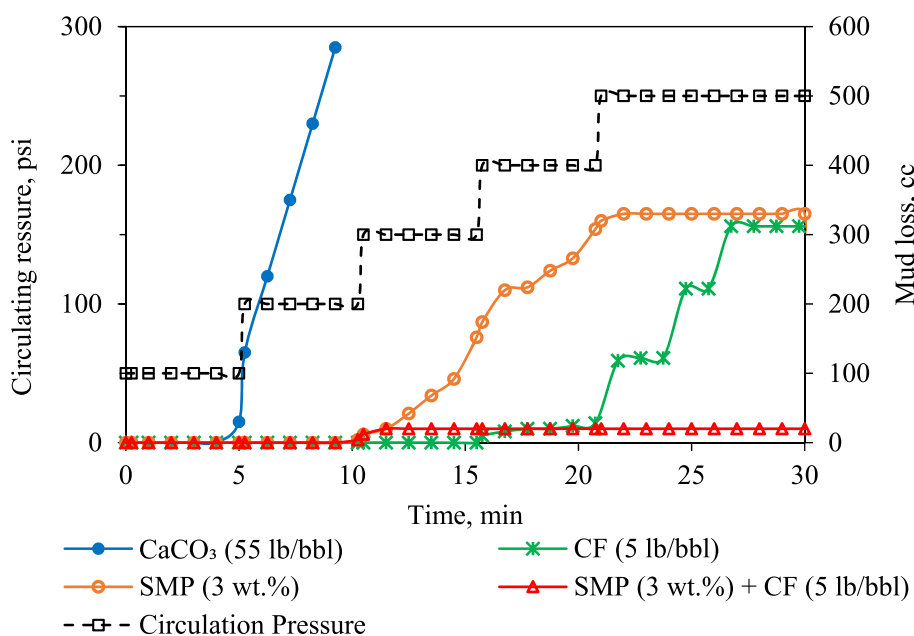


Fig. 8. Mud loss from dynamic testing of LCMs in 1000 μ m fracture.

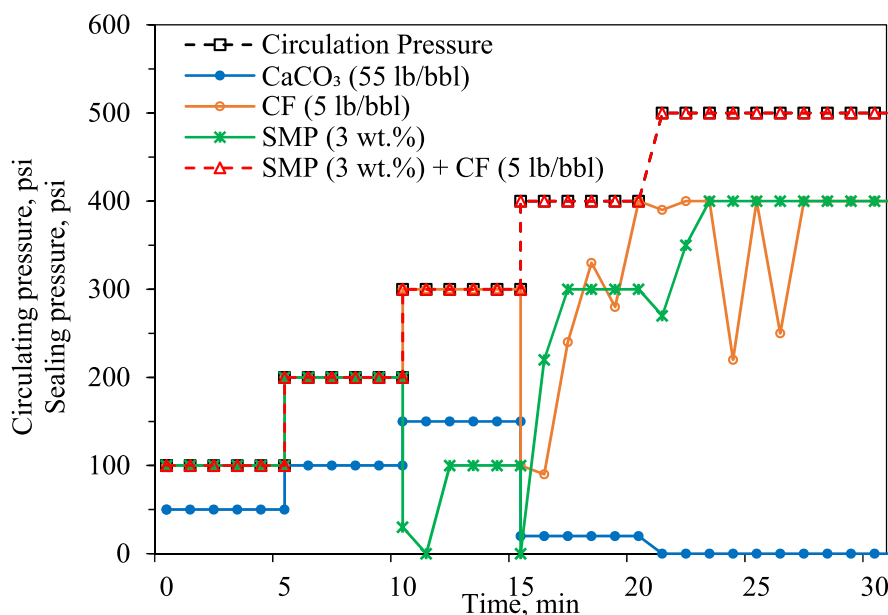


Fig. 9. Sealing pressure from dynamic testing of LCMs in 1000 μm fracture.

was reached. Unlike the results obtained from the static condition, the sealing pressure dropped to 50% at high temperature, and the CF failed in creating a permanent and stable plug, which is reflected in the fluctuation of the sealing pressure, especially at circulating pressures higher than 300 psi.

The presented results also show that the sealing pressure obtained by a 3 wt% SMP mud. The results showed good performance with circulation pressure changes. Although the loss was observed in a lower pressure (100 psi) compared to the CF sealing pressure (300 psi), the sealing was quickly maintained. However, when the circulation pressure was increased to 400, the sealing failed. The SMP could not hold pressure beyond 300 psi; this could be due to the lack of small particles that may potentially fill the gap between the large, activated particles of the SMP. Therefore, the SMP was blended with the CF to form an improved bridged in the fracture's face. The blend shows significant improvement in sealing pressure. On the other hand, the excellent performance of the SMP/CF blend was observed in the sealing pressure verse time, which

showed stable and efficient sealing over all the circulation pressure values.

3.2.2. Sealing integrity in a 3000 μm fracture

Geothermal resources are known to have larger fracture width than those encountered in conventional oil and gas drilling. At the high temperatures in geothermal wells, the size of the fractures becomes more critical. In this study, the effect of fracture size on the performance of LCM is investigated by creating fractures with 3000 μm width. The sealing experiments were conducted using two different concentrations of SMP + CF blends. Two concentrations of 3% SMP and 6% SMP were added to a 5 lb/bbl CF in WBM. The effect of fracture size and LCM concentration on both loss rate and sealing pressure was evident.

Fig. 10 demonstrates how the concentration of SMP affects the mud loss for the larger fractures. The loss rates through the 3000 μm fracture were recorded during the dynamic testing for the two concentrations of SMP in the CF blend. The results showed that with the 3000 μm fracture,

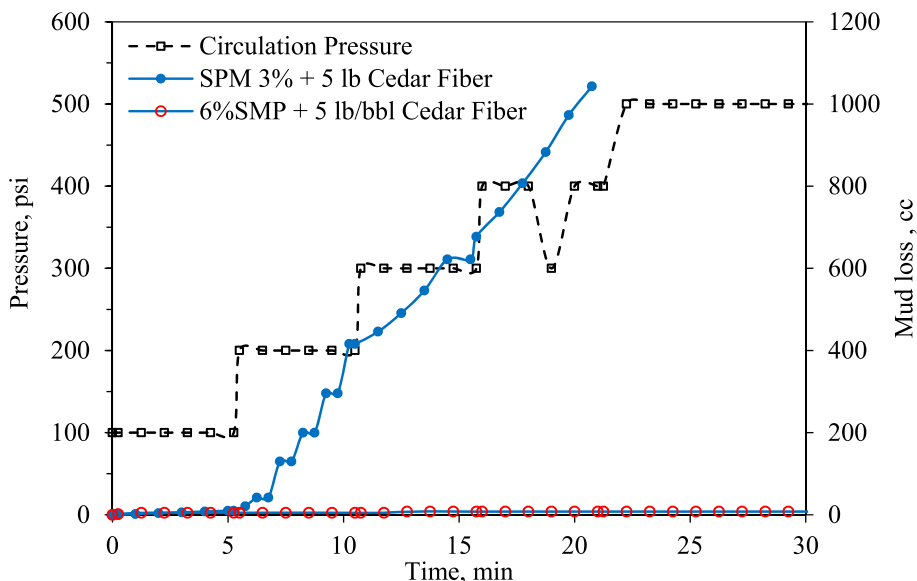


Fig. 10. Mud loss from dynamic LCM testing experiments with 3000 μm fracture.

unlike with the 1000 μm , the lower concentration of 3 wt% SMP + CF failed catastrophically. At only 200 psi circulating pressure, a total loss occurred, and the loss rate as high as 93 cc/min. This weak performance was attributed to the low concentration of SMP in the mud, where the particles were not enough to form a strong plug on the larger fracture opening. To overcome this, the concentration of SMP was increased to 6 wt%, which completely solved the loss problem. As a result, the loss rate became insignificant at the various tested circulating pressure from 100 to 500 psi, and it peaked at less than 10 cc at the end of the test.

Similarly, the pressure monitoring of the time-dependent differential pressures changes across the fracture shown in Fig. 11 reflects the dynamic sealing pressure at every time step. In agreement with the total loss observed with 3 wt%, the sealing pressure started building from a value of 100 psi and increasing in an irregular stepwise fashion with respect to the circulating pressure before it dropped suddenly to zero when circulating pressure exceeded 300 psi. As the sealing pressure drops to zero, the fracture is completely open, and the loss continues for 15 min accumulating more than 1040 cc mud loss. During this period, differential pressure began building from a value of 100 psi and hovered between 100 psi and 200 psi. Therefore, the average sealing pressure was taken to be 100 psi. The mud loss problem was managed when the concentration of the SMP in the LCM blend was increased. For the 6% wt. and cedar fiber mixture, SMP mixed with 5 lb/bbl CF, the mud loss was minimal and constant. Only about 5 cc, which was a direct reflection of the LCM plug status. This concludes that the low concentration of SMP in the mixture with the CF does not perform well when large fractures are encountered.

Fig. 12 shows a tornado plot for the summary of the performances of all the fluids tested in this study in the dynamic high-temperature testing unit. The performance analysis was based on both sealing pressure and mud losses. The maximum sealing pressure that the plug can withstand and the cumulative mud loss can be obtained from the time-dependent results recorded during dynamic mud loss experiments. The major observation in the performance of the SMP + CF blend is that when fracture size increased from 1000 to 3000 μm , the mud loss increased by 130%. The 6% wt. SMP mixture significantly improves the sealing pressure up to 500 psi. The high concentration of the SMP also reduced the mud losses through the fracture opening down to 8 cc. These improvements relate to the concentrated larger particle size of the SMP, which increases the integrity of the seal.

From the preceding results of the static filtration test, the positive effect of SMP on loss control through a fractured disk was evident. Moreover, the dynamic flow loop simulator helps in better evaluating the LCM's performance at high temperatures on a larger scale under dynamic conditions. In the static filtration test with the PPA, the disk is only 6.35 mm thick which represents the depth or the length of the fracture. Therefore the ratio of fracture size to the fracture length is very small and not representative of the actual sealing mechanisms of granular LCM. The bridging on the fracture is not representative of the actual drilling conditions. The static test also ignores the effect of circulation, shearing, and filter cake erosion which is counted for in the dynamic flow loop, which allows circulating of the drilling fluid while radial filtration is occurring and filter LCM plug is being established. These variations in testing conditions reflected on the results where the static filtration results showed high performance for the SMP at the maximum tested differential pressure (500 psi) without much information on how and when the seal occurs. Also, the cedar fiber failed during the static filtrations at 200 psi. In contrast, dynamic filtration tests showed that the cedar fiber could reform a plug on the fracture opening with sealing pressure up to 300 psi due to the continuous flow of cedar fiber across the fracture.

In the dynamic testing flow loop, the LCM's mud is circulated beneath the fracture at predetermined circulating pressure. Then, the downstream valve is opened to encourage the flow into the fracture. The results of the different LCM formulations showed that the flow of the mud into the fracture opening (1000 and 3000 μm) and through the fracture length (13.5 inches) depends on the type, the concentration of the LCMs and the size of the fracture, besides the temperature and circulating pressure.

Another major observation is that although SMP stands alone reduced the mud loss, the sealing pressure was not stable. This can be attributed to the nature of particulate SMP, which governs its bridging mechanism. The SMP + Fiber blend forms a better rigid plug on the fracture opening because the fiber is known for its mat-like bridging, which fills the voids that may exist in the SMP bridge. Finally, to overcome the impact of large fracture size and high temperature, a high concentration of SMP is recommended, about 6 wt%.

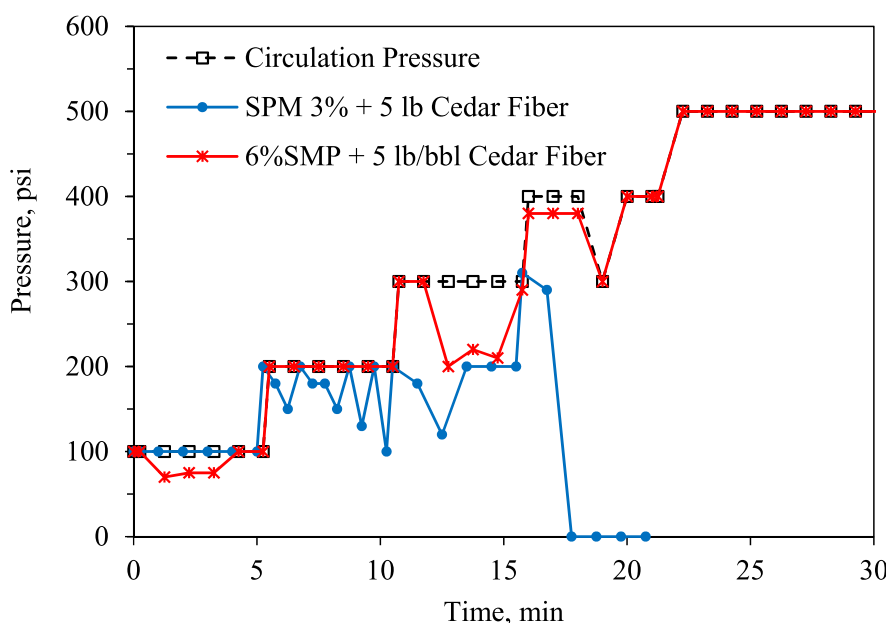


Fig. 11. Sealing pressure from the dynamic LCM testing experiments with 3000 μm fracture.

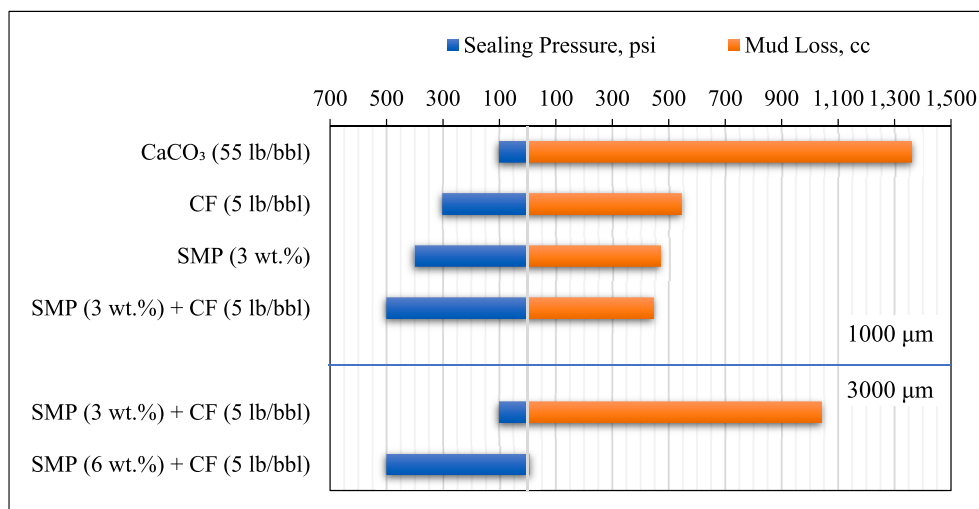


Fig. 12. Summary plot of the dynamic LCM testing for sealing pressure and mud loss.

4. Conclusion

Wellbore strengthening with the right selection and concentration of LCM in drilling fluids may decrease the mud loss problems in geothermal wells drilling, which reduces non-productive time. In this paper, we examined different LCM performance in sealing different fracture sizes using both static filtration and a novel dynamic LCM testing unit. This high-temperature dynamic testing flow loop provides a tool to test loss circulation materials under high-temperature conditions and under dynamic conditions with variable circulation rates of drilling mud. The setup accommodates actual rock cores with various fracture lengths up to 14 inches. Valuable information can be extracted to help to evaluate the performance and success rate of loss circulation materials during geothermal drilling.

The following are the key findings:

- In the static filtration, the sealing efficiency of the cedar fiber outperformed the CaCO₃. Cedar fiber reduced fluid loss by more than 89% and increased sealing pressure to 200psi.
- Shape memory polymers showed more significant potential and performance in sealing fracture with different sizes compared to conventional LCMs such as cedar fiber and calcium carbonate.
- The 6% weight SMP blend performed better in plugging the large 3000 μm fracture than 3% weight SMP blend. Thus, increasing the weight concentration of the SMP as the fracture sizes get larger improves the sealing efficiency of the SMP.
- The dynamic testing unit offers a better tool and more excellent reliability in testing LCMs at elevated temperatures than static filtration or permeability plugging testing.

Authors declaration of interest statement

We the undersigned declare that this manuscript is original, has not been published before and is not currently being considered for publication elsewhere.

We wish to confirm that there are no known conflicts of interest associated with this publication and there has been no significant financial support for this work that could have influenced its outcome.

We confirm that the manuscript has been read and approved by all named authors and that there are no other persons who satisfied the criteria for authorship but are not listed. We further confirm that the order of authors listed in the manuscript has been approved by all of us.

We confirm that we have given due consideration to the protection of intellectual property associated with this work and that there are no

impediments to publication, including the timing of publication, with respect to intellectual property. In so doing we confirm that we have followed the regulations of our institution concerning intellectual property.

We understand that the Corresponding Author is the sole contact for the Editorial process (including Editorial Manager and direct communications with the office). He is responsible for communicating with the other authors about progress, submissions of revisions and final approval of proofs. We confirm that we have provided a current, correct email address which is accessible by the Corresponding Author and which has been configured to accept email from eesserver@eesmail.elsevier.com.

Declaration of competing interest

The authors declare that they have no known competing financial interests or personal relationships that could have appeared to influence the work reported in this paper.

Acknowledgment

The authors would like to thank the U.S. Department of Energy Office of Energy Efficiency and Renewable Energy (EERE) under the Geothermal Program Office Award Number DE-EE0008602 for this research grant.

References

- Alsaba, Mortadha, Nygaard, Runar, Hareland, Geir, Contreras, Oscar, 2014. Review of lost circulation materials and treatments with an updated classification. InAADE National Technical Conference and Exhibition, Houston, pp. 1–9, 2014 Apr 15.
- Brandl, A., Bray, W.S., Molaei, F., 2011. Curing Lost Circulation Issues and Strengthening Weak Formations with a Sealing Fluid for Improved Zonal Isolation of Wellbores. Australian Geothermal Energy Conference, Melbourne.
- Bauer, S., Gronewald, P., Hamilton, J., LaPlant, D., Mansure, A., 2005. High-Temperature Plug Formation with Silicates, SPE International Symposium on Oilfield Chemistry. The Woodlands, Texas, 2 February.
- Bauer, S.J., Galbreath, D., Hamilton, J., Mansure, A.J., 2004. Comments on high temperature plugs: progress report on polymers and silicates. *Trans. Geoth. Resour. Counc.* 28, 145–152.
- Contreras, O., Hareland, G., Husein, M., Nygaard, R., Alsaba, M., 2014. Wellbore Strengthening in Sandstones by Means of Nanoparticle-Based Drilling Fluids." the SPE Deepwater Drilling and Completions Conference. Galveston, Texas, USA. <https://doi.org/10.2118/170263-MS>. September 2014.
- Cook, J., Growcock, F., Guo, Q., Hodder, M., van Oort, E., 2012. Stabilizing the wellbore to prevent lost circulation. *Oilfield Rev.* 23 (4), 26–35.
- Dobson, P.F., et al., 2021. Fracture sustainability in enhanced geothermal systems: experimental and modeling constraints. *J. Energy Resour. Technol.* 143 (10).

- Dumas, P., Antics, M., Ungemach, P., 2013. Report on Geothermal Drilling. Accessed on March 2013. <http://www.geoelec.eu/wp-content/uploads/2011/09/D-3.3-G-EOELEC-report-on-drilling.pdf>.
- Ezeakacha, C.P., Salehi, S., 2019. A holistic approach to characterize mud loss using dynamic mud filtration data. *J. Energy Resour. Technol.* 141 (7).
- Ekeoma, Isaac, P., Dosunmu, Adewale, Anyanwu, Chimaroke, 2019. Laboratory study of oil palm kernel shells and mangrove plant fiber, bana trunk fiber as lost circulation materials in synthetic based drilling mud. The SPE Nigeria Annual International Conference and Exhibition, Lagos, Nigeria. <https://doi.org/10.2118/198733-MS>. August 2019.
- Fan, Jizhou, Li, Guoqiang, 2018. High enthalpy storage thermoset network with giant stress and energy output in rubbery state. *Nat. Commun.* 9, p642.
- Fan, Jizhou, Santos, L.Y., Taleghani, A.D., Li, G., 2020. Stimuli-responsive petroleum cement composite with giant expansion and enhanced mechanical properties. *Construct. Build. Mater.* 259, p119783. <https://doi.org/10.1016/j.conbuildmat.2020.119783>.
- Feng, Yongcun, Gray, K.E., 2018. *Lost Circulation and Wellbore Strengthening*. Springer International Publishing; 2018 May 1.
- Finger, John, Blankenship, Doug, 2010. *Handbook of Best Practices for Geothermal Drilling*, 2010. Sandia National Laboratories, Albuquerque.
- Fridheim, J.E., Arias-Prada, J.E., Sanders, M.W., Shursen, R., 2012. Innovation Fiber Solution for Wellbore Strengthening." IADC/SPE Drilling Conference and Exhibition. San Diego Jan 1, p. 9.
- Gianelli, G., Manzella, A., Puxeddu, M., 1997. Crustal models of the geothermal areas of southern Tuscany (Italy). *Tectonophysics* 281 (3–4), 221–239.
- Hamza, A., Shamlooh, M., Hussein, I.A., Nasser, M., Salehi, S., 2019. Polymeric formulations used for lost circulation materials and wellbore strengthening applications in oil and gas wells: a review. *J. Petrol. Sci. Eng.* 180, 197–214.
- Hanano, M., 2000. Two Different Roles of Fractures in Geothermal Development Proceedings World Geothermal Congress. Kyushu - Tohoku, Japan. May 28 - June 10. https://www.researchgate.net/publication/265924852_Two_different_roles_of_fractures_in_geothermal_development.
- Javeri, S.M., Haindade, Z.M.W., Jere, C.B., 2011. Mitigating Loss Circulation and Differential Sticking Problems Using Silicon Nanoparticles, SPE/IADC Middle East Drilling Technology Conference and Exhibition. Society of Petroleum Engineers, Muscat, Oman, p. 4.
- Jing, L., Stephansson, O., 1997. Network topology and homogenization of fractured rocks, 1997. In: Jamtveit, B., Yardley, B.W. (Eds.), *Fluid Flow and Transport in Rocks – Mechanisms and Effects*. Chapman & Hall, pp. 191–202.
- Lee, L., Taleghani, A.D., 2020. Looking at Fracture Sealing Mechanisms by Granular LCM at Elevated Temperatures. Stanford Geothermal Workshop, Stanford, California, USA.
- Lendlein, A., Kelch, S., 2002. Shape-memory polymers. *Angew. Chem. Int. Ed.* 41 (12), 2034–2057.
- Liu, Y., Du, H., Liu, L., Leng, J., 2014. Shape memory polymers and their composites in aerospace applications: a review. *Smart Mater. Struct.* 23 (2), 023001.
- Loeppeke, G., 1986. *Evaluating Candidate Lost Circulation Materials for Geothermal Drilling*. Sandia National Labs., Albuquerque, NM (USA).
- Magzoub, M.I., Salehi, S., Hussein, I., Nasser, M., 2021a. Development of a polyacrylamide-based mud formulation for lost circulation treatments. *J. Energy Resour. Technol.* 143 (7).
- Loeppeke, Gelan E., Glowka, David A., Wright, Elton K., 1990. Design and evaluation of lost-circulation materials for severe environments. *J. Petrol. Technol.* 3 (42), 328–337. <https://doi.org/10.2118/18022-PA>.
- Magzoub, M.I., Salehi, S., Hussein, I.A., Nasser, M.S., 2020. A comprehensive rheological study for a flowing polymer-based drilling fluid used for wellbore strengthening. SPE International Conference and Exhibition on Formation Damage Control. Society of Petroleum Engineers, Lafayette, Louisiana.
- Magzoub, Musaab, Salehi, Saeed, Li, Guoqiang, Fan, Jizhou, Teodoriu, Catalin, 2021b. Loss circulation prevention in geothermal drilling by shape memory polymer, 89. *Geothermics* (Elsevier).
- Mansour, Khaled A., Taleghani, Dahi A., 2018. Smart Loss Circulation Materials for Drilling Highly Fractured Zones." SPE/IADC Middle East Technology Conference and Exhibition. Abu Dhabi, UAE. <https://doi.org/10.2118/189413-MS>.
- Mansour, A., Taleghani, A.D., Salehi, S., Li, G., Ezeakacha, C., 2019. Smart lost circulation materials for productive zones. *Journal of Petroleum Exploration and Production Technology* 9 (1), 281–296.
- Mietta, F., Chassagne, C., Manning, A.J., Winterwerp, J.C., 2009. Influence of shear rate, organic matter content, pH and salinity on mud flocculation. *Ocean Dynam.* 59 (5), 751–763.
- Miranda, M.M., et al., 2018. Fracture Network Characterization as Input for Geothermal Energy Research: Preliminary Data from Kuujuaq, Northern Québec, Canada, Proceedings 43rd Workshop on Geothermal Reservoir Engineering. Stanford, California, p. 12.
- Mudgal, K., Ghorai, P., 2015. A review: improvement in the methods for controlling of shape memory alloy actuator during the last decade. *Sens. Lett.* 13 (6), 439–448.
- Salih, A., Bilgesu, H., 2017. Investigation of Rheological and Filtration Properties of Water-Based Drilling Fluids Using Various Anionic Nanoparticles, SPE Western Regional Meeting. Society of Petroleum Engineers.
- Salehi, S., Nygaard, R., 2011. Evaluation of New Drilling Approach for Widening Operational Window: Implication for Wellbore Strengthening." the SPE Production and Operations Symposium. Oklahoma City, Oklahoma, USA. <https://doi.org/10.2118/140753-MS>. March 27.
- Schild, M., Vollbrecht, A., Siegesmund, S.t., Reutel, C., 1998. Microcracks in granite cores from the EPS-1 geothermal drill hole, Soultz-sous-Forêts (France): paleostress directions, paleofluids and crack-related Vp-anisotropies. *Geol. Rundsch.* 86 (4), 775–785.
- Seifollahi, S., Dowd, P.A., Xu, C., 2014. An enhanced stochastic optimization in fracture network modelling conditional on seismic events, 2014 *Comput. Geotech.* 61, 85–95.
- Singhal, B.B.S., Gupta, R.P., 2010. *Applied Hydrogeology of Fractured Rocks*, 2010. Springer, p. 429.
- Taleghani, D.A., Li, G., Moayeri, M., 2017. Smart expandable cement additive to achieve better wellbore integrity. *J. Energy Resour. Technol.* p7.
- Vidal, J., Genter, A., Chopin, F., 2017. Permeable fracture zones in the hard rocks of the geothermal reservoir at Rittershoffen, France. *J. Geophys. Res.: Solid Earth* 122 (7), 4864–4887. <https://doi.org/10.1002/2017jb014331>.
- Villa, I.M., Ruggieri, G., Puxeddu, M., Bertini, G., 2006. Geochronology and isotope transport systematics in a subsurface granite from the Larderello–Travale geothermal system (Italy). *J. Volcanol. Geoth. Res.* 152 (1–2), 20–50.
- Zhong, H., et al., 2019. Minimizing the HTHP filtration loss of oil-based drilling fluid with swellable polymer microspheres. *J. Petrol. Sci. Eng.* 172, 411–424.